RESEARCH ARTICLE

Stepwise Construction of Supramolecular A_2B_4-type Miktoarm Star Copolymers with a Cobalt Phthalocyanine Core

Xinhao Zhong,[a,b] Hsu-Tzu Cheng,[c] Chu-Chen Chueh,[c] Masayuki Takeuchi*,[a,b,d,e] and Junko Aimi*[a]

[a] X. Zhong, Prof. M. Takeuchi, Dr. J. Aimi
Research Center for Macromolecules and Biomaterials, 1-2-1 Sengen, Tsukuba, Ibaraki, 305-0032, Japan
National Institute for Materials Science: NIMS
1-2-1 Sengen, Tsukuba, Ibaraki, 305-0032, Japan
E-mail: AIMI.Junko@nims.go.jp; TAKEUCHI.Masayuki@nims.go.jp

[b] X. Zhong, Prof. M. Takeuchi
Department of Materials Science and Engineering
University of Tsukuba
1-1-1 Tennodai, Tsukuba, Ibaraki, 305-8577, Japan

[c] H.-T. Cheng, Prof. C.-C. Chueh
Department of Chemical Engineering
National Taiwan University

[d] Prof. M. Takeuchi
Research Center for Autonomous Systems Materialogy (ASMat), Institute of Integrated Research (IIR),
Institute of Science Tokyo (Science Tokyo)

[e] Prof. M. Takeuchi
Institute of Mutidisciplinary Research for Advanced Materials,
Tohoku University

Supporting information for this article is given via a link at the end of the document.

Abstract: Supramolecular interactions between polymers play a crucial role in the construction of three-dimensional polymer structures with unique physical and chemical properties. In this study, we have fabricated a novel supramolecular miktoarm star copolymer (μ-star) with a cobalt(II) phthalocyanine (CoPc) core using metal–ligand coordination. Axial coordination of the terminal pyridyl group of poly(methyl methacrylate) with the CoPc core of four-armed star-shaped polystyrene provided AB_4- and A_2B_4-type μ-stars through stepwise complexation. The spin-coated polymer films from mixed solutions of $CoPcPS_4$ and pyPMMA in 1:1 or 1:2 mass ratios exhibited phase-separated nanodomains with smooth surfaces. Supramolecular interactions in polymer systems provide a unique topology to polymers and affect their bulk morphology.

Introduction

Supramolecular polymers formed through noncovalent interactions are regarded as important materials because of their dynamic nature, which allows them to adapt to environmental changes.[1] In addition, the versatility of their building blocks imparts them with various physical and chemical properties.[2] In particular, the incorporation of π-conjugated aromatic molecules such as porphyrins and phthalocyanines into the supramolecular systems results in unique optical and electrical properties that enhance their applicability in biomaterials and organic electronics.[3] Recently, we had prepared supramolecular miktoarm star copolymers (μ-stars), composed of star-shaped polystyrene with a zinc phthalocyanine core ($ZnPcPS_4$) and pyridyl end-functionalized polymers (py-polymer).[4] These asymmetric polymers with functional cores are synthetic targets, and their synthesis typically requires multiple steps.[5] In contrast, supramolecular interactions between the core and polymer can be used to create μ-stars by simply mixing the components.[6] In our previous study, we demonstrated the formation of the AB_4-type supramolecular μ-stars with various arm polymer constitutions via the coordination interaction between ZnPc and pyridine-tethered polymers.[4] Furthermore, the supramolecular μ-stars having ZnPc core showed unique phase-separated morphology in thin films, exhibiting excellent charge-trapping ability for the organic field-effect transistor (OFET) memory device applications.[7]

In this study, we prepared supramolecular μ-stars with a cobalt(II) phthalocyanine (CoPc) core, where the AB_4- and A_2B_4- type μ-stars were formed through axial coordination of py-polymer in a stepwise manner. CoPc derivatives have been widely studied as molecular catalysts,[8] and it has been shown that axially coordinating polymers to these CoPc derivatives enhance the activity and selectivity of electrochemical CO_2 reduction by tuning the catalytic environment around the CoPc molecule.[9] Complexation events were comprehensively investigated using UV-Vis and ^{1}H NMR titration experiments. Additionally, the

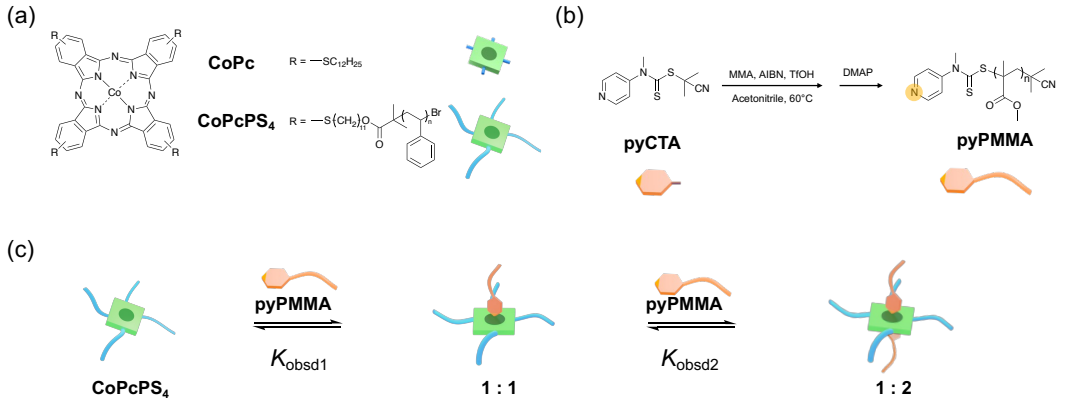

Figure 1. a) Chemical structures of CoPc derivatives. b) Synthesis of pyridyl-terminated **pyPMMA.** c) Schematic illustration of the construction of supramolecular μ-stars with a CoPc core.

surface morphology of the supramolecular μ-stars in the thin-film state was characterized by atomic force microscopy (AFM) analyses. The proposed supramolecular strategy enables the preparation of μ-stars with diverse nanostructures, which provides a versatile platform for designing functional materials with potential applications in optoelectronic devices.

Results and Discussion

Four-armed star-shaped polystyrene with a CoPc core was synthesized via a procedure similar to that for ZnPc or CuPc cores (**Figure 1a**).[10] Phthalonitrile (Pn)-terminated polystyrene (PnPS) with a number-average molecular weight (M_n) of 4.0 kg mol^{-1} and a polydispersity index (PDI) of 1.04, which was reported in the previous study,[4] was used for the cyclization reaction with cobalt chloride ($CoCl_2$) in the presence of 1,8-diazabicyclo[5.4.0]undec-7-ene (DBU) in 1-pentanol. The product was purified by preparative recycling gel permeation chromatography (GPC), resulting in a four-armed star-shaped polymer with a CoPc core (**CoPcPS$_4$)** with M_n of 14.1 kg mol^{-1} and PDI of 1.10. Cobalt(II) tetrakis-[(dodecyl)thio]phthalocyanine (**CoPc**) was also synthesized for comparison via the cyclization of 4-dodecylthio-1,2,-dicyanobenzene with $CoCl_2$ under basic conditions using DBU. Poly(methyl methacrylate) with a pyridyl end group (**pyPMMA**) was synthesized by reversible addition–fragmentation chain transfer (RAFT) polymerization using a chain transfer agent containing a pyridyl group, 2-cyanopropan-2-yl N-methyl-N-(pyridin-4-yl)carbamodithioate (**pyCTA**),[11] aiming to construct a supramolecular complex, as shown in **Figure 1b, c**. The synthetic procedures in detail were reported in our previous study.[4] All polymers used in this study are summarized in **Table 1**.

Supramolecular complexation of the pyridyl groups of the py-tethered polymers and CoPc derivatives was investigated using UV–visible absorption spectroscopy. To analyze the interaction between the CoPc core and the pyridyl group of the CTA derivatives, we first examined a model system using **CoPc** and **pyCTA**. The absorption spectrum of **CoPc** in toluene showed a characteristic absorption band at approximately 350 nm, referred to as the Soret band, and a strong Q-band in the range 600–800 nm (**Figure S1)**. In contrast, **pyCTA** exhibited a broad absorption band at approximately 300 nm (**Figure S2**). When a toluene solution of **pyCTA** was added to **CoPc** in toluene, the absorption peak at 685 nm decreased and shifted slightly to shorter wavelengths, whereas the shoulder peak at 670 nm increased, with an isosbestic point at 678 nm (**Figure 2a, blue lines**). This indicates the formation of the **CoPc-pyCTA** complex through

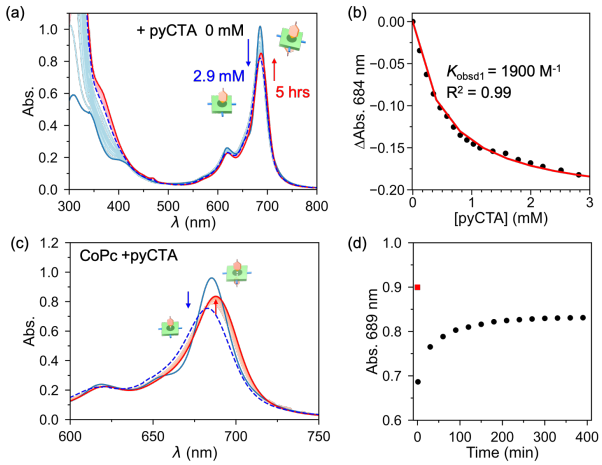

Figure 2. a) Absorption spectral changes of **CoPc** upon the gradual addition of **pyCTA** in toluene at 25 ˚C. b) Plot of absorbance at 684 nm (dots) with a fitted curve based on the 1:1 binding model (red line). c) Absorption spectral changes after mixing **CoPc** and **pyCTA**. d) Time-course measurements of absorbance at 689 nm of **CoPc** before (red square) and after (black dots) mixing with **pyCTA**.

Table 1. Characteristics of the polymers.

Polymer	M_n (g/mol)[a]	PDI[a]	DP[b]
CoPcPS$_4$	14 100	1.10	38 (each arm)
pyPMMA	13 900	1.16	132
PMMA	14 000	1.15	133

[a] Number average molecular weight and polydispersity index determined by GPC analysis with polystyrene standards. [b] Estimated degree of polymerization (DP) based on the M_n from GPC.

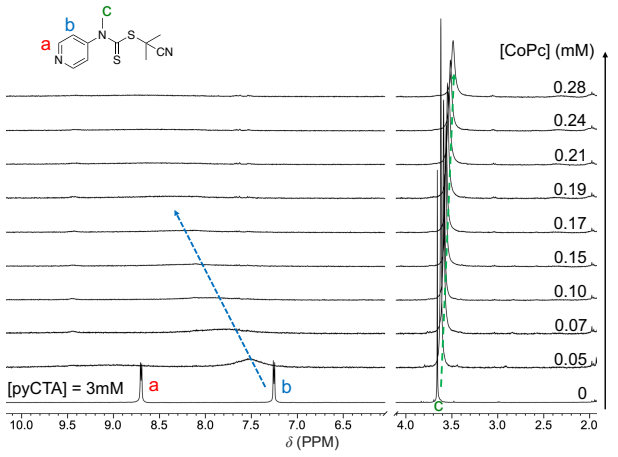

Figure 3. ^{1}H NMR spectral changes of **pyCTA** upon the addition of **CoPc** in CD_2Cl_2.

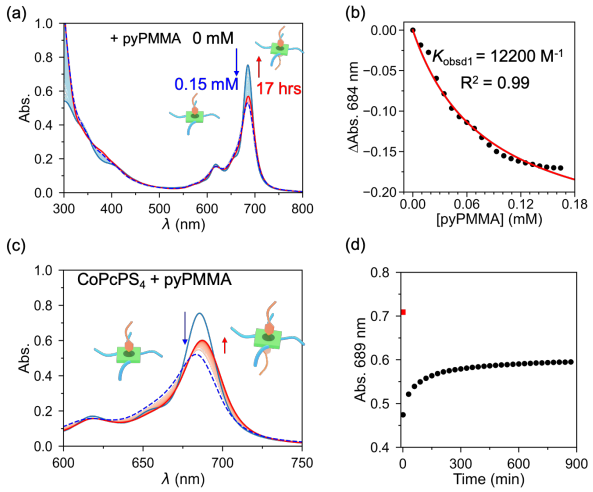

Figure 4. a) Absorption spectral changes of **CoPcPS$_4$** upon the gradual addition of **pyPMMA** in toluene at 25 ˚C. b) Plot of absorbance at 684 nm (dots) with a fitted curve based on the 1:1 binding model (red line). c) Absorption spectral changes after mixing **CoPcPS$_4$** and **pyPMMA.** d) Time course measurements of absorbance at 689 nm of **CoPcPS$_4$** before (red square) and after (black dots) mixing with **pyPMMA**.

metal–ligand coordination. Excess addition of **pyCTA** (up to 2.9 mM) to the **CoPc** solution (20 μM) almost eliminated the spectral change. Interestingly, when we continued to monitor the spectrum, the absorption peak of the Q-band slowly increased with time, with a gradual redshift over 5 h (**Figure 2a, red lines**). This change was accompanied by a new isosbestic point at 684 nm, suggesting the existence of an equilibrium distinct from the initial equilibrium. It is most likely that a 1:1 complex of **CoPc** and **pyCTA** formed initially was followed by the coordination of the second **pyCTA** from the opposite side of the CoPc plane at a slower rate. To investigate the detailed time course, UV-vis absorption spectra were monitored every 30 min after mixing **CoPc** (15 μM) with a large excess of **pyCTA** (6 mM) in toluene (**Figure 2c**). The absorption peak in the Q band decreased immediately after the addition of **pyCTA**, followed by a gradual increase. When the absorbance was plotted at 689 nm, a gradual increase was observed over a period of approximately 5 h (**Figure 2d**). A similar stepwise absorption change was observed in the ligand exchange of DMSO and pyridine for the coordination of **CoPc** derivative.[12] The addition of **pyCTA** to the **CoPc** solution proceeded via a two-step process, forming a 1:1 coordination, followed by a slower 1:2 coordination. The slow rate of 1:2 complexation may be attributed to the cobalt ion in the 1:1 complex being displaced out-of-the-plane of the phthalocyanine ring owing to its interaction with the **pyCTA** ligand.[13] The distortion of **CoPc(pyCTA**) may make a second axial coordination of **pyCTA** from the opposite side of the plane difficult. Because the 1:2 coordination was time dependent, only the observed association constant (K_{obsd1}) value was estimated by fitting the absorbance change at 684 nm to a 1:1 binding equation. Notably, the absorbance at 684 nm corresponds to the isosbestic point for the formation of the 1:2 complex. Therefore, the potential influence of the 1:2 coordination was neglected in the calculation of K_{obsd1}, and the value was estimated to be 1.9×10^3 M^{-1} in toluene (**Figure 2b)**. This K_{obsd1} value is twice that of the ZnPc-pyCTA complex reported in a previous study.[4]

The supramolecular interactions between **CoPc** and **pyCTA** were examined using ^{1}H NMR spectroscopy. The ^{1}H NMR spectrum of **CoPc** showed only a broad signal owing to the paramagnetic nature of the Co(II) complex (**Figure S3**). Therefore, we conducted ^{1}H NMR titration analyses by adding a solution of **CoPc** to the **pyCTA** solution, which is the reverse of the titration procedure used in UV–visible absorption spectroscopy. When a solution of CoPc was added to **pyCTA** in deuterated dichloromethane (CD_2Cl_2), the proton signals of the pyridyl group of **pyCTA** (H^a, H^b) rapidly broadened and disappeared owing to the paramagnetic effect of the Co(II) complex (**Figure 3**). In contrast, the *N*-methyl group of **pyCTA** proton signal (H^c) shifted from 3.65 to 3.48 ppm. These results indicate that the **pyCTA** protons were affected by the ring current of the aromatic CoPc core through the axial coordination of **pyCTA** to **CoPc**, confirming the formation of a supramolecular complex.

Following the observation of supramolecular interactions between **CoPc** and **pyCTA** derivatives, we investigated the polymer systems using absorption spectroscopy. The absorption spectrum of the newly synthesized **CoPcPS$_4$** was similar to that of **CoPc** in toluene, confirming that the CoPc core in the star polymer has the same electronic structure as that of the surrounding polymer chains (**Figure S1**). When the **pyPMMA** solution was added to the toluene solution of **CoPcPS$_4$**, the absorption peak at 685 nm first decreased. This phenomenon was almost identical to that **CoPc-pyCTA** complexation in toluene, indicating the formation of a 1:1 complex between **CoPcPS$_4$** and **pyPMMA (Figure 4a, blue lines)**. However, only a small spectral change, caused by the dilution, was observed when a toluene solution of PMMA without a pyridyl unit was added to the **CoPcPS$_4$** solution (**Figure S4ab**). Therefore, the pyridyl end group of **pyPMMA** appeared to coordinate with the CoPc core of **CoPcPS$_4$**. The K_{obsd1} value for the 1:1 association between **CoPcPS$_4$** and **pyPMMA** was evaluated to be 1.2×10^4 M^{-1} in toluene (**Figure 4b**).[14] After the addition of 0.15 mM of **pyPMMA**, the solution was continuously monitored and a gradual increase in absorbance at 700 nm with a new isosbestic point at 684 nm was observed **(Figure 4a, red lines)**. This implies an alternative coordination of **pyPMMA** to the

CoPc core, as seen in the case of **CoPc-pyCTA** systems. The absorption spectra of a mixture of **CoPcPS$_4$** and **pyPMMA** were measured every 30 min. The Q-band absorption of **CoPcPS$_4$** decreased immediately and then slowly increased over 10 h in toluene **(Figure 4c, d)**. This spectral change appeared to be slower than that observed for the mixture of **CoPc** and **pyCTA** (**Figure S5**). These results confirmed the stepwise formation of the A_2B_4-type supramolecular *μ*-stars via metal–ligand coordination between the pyridyl group of pyPMMA and the CoPc core of the star polymer.

The film morphology of the resulting supramolecular *μ*-stars was investigated by AFM. A flat, smooth surface was observed in the AFM height image of **CoPcPS$_4$** (**Figure S6**). Polymer films were then prepared by spin coating mixed solutions of **CoPcPS$_4$** and **pyPMMA** in 1:1 and 1:2 mass ratios. Because the M_n of **pyPMMA** is similar to that of **CoPcPS$_4$**, their molar ratios were also considered to be approximately 1:1 and 1:2, corresponding to 1:1 and 1:2 complexation between **CoPcPS$_4$** and **pyPMMA**. Considering the slow rate of complexation, mixed solutions of **CoPcPS$_4$** and **pyPMMA** were stirred overnight at room temperature before spin coating. As shown in **Figure 5**, the 1:1 and 1:2 blend films spin-coated from CH_2Cl_2 solutions exhibited distinct phase-separated morphologies in the AFM height images. The height image of the 1:1 **CoPcPS$_4$-pyPMMA** film showed a dispersed droplet-type phase-separated morphology with sizes between 50–80 nm (**Figure 5a**), whereas the 1:2 **CoPcPS$_4$-pyPMMA** film showed worm-like structures (**Figure 5b**). The root-mean-square (RMS) surface roughness (Rq) of the **CoPcPS$_4$-pyPMMA** blended polymer films was estimated to be 1.15 nm and 1.28 nm for 1:1 and 1:2 blends, respectively. Binary polymer blends of PS and PMMA normally exhibit phase-separated structures on the macroscale owing to the strong phase segregation between immiscible polymers.[15] In addition, the blended films of **CoPcPS$_4$** and PMMA without a pyridyl end group were prepared, which exhibited irregular phase-separated structures in macroscale unlike the **CoPcPS$_4$-pyPMMA** films (**Figure S7**).

The polymer films with supramolecular *μ*-stars showed microdomains with relatively smaller Rq values, implying the influence of coordination between two polymer segments. To investigate the metal–ligand coordination inside the polymer films, we measured their UV-Vis absorption spectra. As shown in **Figure S8**, the **CoPcPS$_4$** film exhibited a bimodal absorption in the Q-band region, suggesting that the CoPc core formed aggregates through π-π interactions in the polymer matrix. The blended film of **CoPcPS$_4$** and PMMA without a pyridyl group exhibited an absorption spectrum similar to that of the **CoPcPS$_4$** film, indicating the presence of CoPc aggregates. In contrast, the **CoPcPS$_4$-pyPMMA** blended film showed a sharper peak, similar to that of the solution state. These results suggest that the aggregation of the CoPc core was hindered in the blend with **pyPMMA**, providing evidence of metal–ligand coordination in the thin film state. Therefore, the smaller phase-separated domains of the polymer blend with smooth surfaces may be derived from coordination interactions between immiscible polymers that act as compatibilizers.

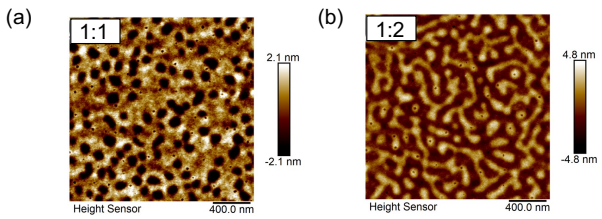

Figure 5. AFM height images of blended films of (a) 1:1 **CoPcPS$_4$-pyPMMA** and (b) 1:2 **CoPcPS$_4$-pyPMMA** spin-coated from CH_2Cl_2 solutions.

The differential scanning calorimetry profile of supramolecular μ-star (1:1 **CoPcPS$_4$-pyPMMA**) showed two distinct glass transistion temperatures (T_g) at 83 ˚C and 117 ˚C, which were derived from **CoPcPS$_4$** and **pyPMMA**, respectively (**Figure S9**). In supramolecular *μ*-star, no transition that is characteristic to the liquid crystalline CoPc core was observed, confirming phase-separation of the polymer mixture without large domains of CoPc aggregates. The morphological differences between the 1:1 and 1:2 **CoPcPS$_4$-pyPMMA** blend films are still under discussion; however, it could be attributed to the early spinodal decomposition of varying proportions of **pyPMMA**.[16] The original supramolecular *μ*-star structures, whether AB_4- or A_2B_4-type, exhibited different three-dimensional structures, which influenced the phase-separated morphology of the blend films prepared by rapid evaporation of the solvents.

Conclusion

We successfully demonstrated the supramolecular complexation of a CoPc derivative with a pyridyl-terminated molecule. The stepwise formation from 1:1 to 1:2 complexation via metal–ligand coordination between CoPc and the pyridyl group was observed in the solution state. The supramolecular interaction between CoPc-cored star-shaped polystyrene and pyridyl-tethered poly(methyl methacrylate) was further investigated using absorption spectroscopic measurements, revealing the formation of AB_4- and A_2B_4-type supramolecular *μ*-stars. In addition, the morphologies of the 1:1 and 1:2 complex polymer blends were examined, revealing phase-separated microdomains in the film state. Altering the central metal ion of the phthalocyanine core of star-shaped polymers provides a new strategy for fabricating topological polymers by axial coordination and obtains microstructures in various combinations of polymer blends. Designing macromolecular architectures containing CoPc and investigating their axial coordination behavior may provide valuable insights for various applications, including optoelectronics and advanced catalytic systems.

Supporting Information

Additional supporting information can be found online in the Supporting Information section at the end of this article.

Acknowledgements

This work was supported by JSPS KAKENHI (Grant No. JP 21K05220 for J. A., 24K01475 and 24K21722 for M. T.), Grant-in-Aid for Transformative Research (A) "Condensed Conjugation" (No. JP20H05868 for M.T.), and a MEXT "NIMS Molecule and Material Synthesis Platform" program. We thank Ms. Izumi Matsunaga and Ms. Bo Zhou for technical supports.

Keywords: miktoarm star copolymer • cobalt phthalocyanine • supramolecular polymers • polymer blend

[1] a) A. W. Bosman, R. P. Sijbesma, E. W. Meijer, *Mater. Today* **2004**, *7*, 34; b) T. Aida, E. W. Meijer, S. I. Stupp, *Science* **2012**, *335*, 813; c) X. Ma, H. Tian, *Acc. Chem. Res.* **2014**, *47*, 1971.

[2] a) O. Ikkala, G. ten Brinke, *Science* **2002**, *295*, 2407; b) Q. Wang, J. L. Mynar, M. Yoshida, E. Lee, M. Lee, K. Okuro, K. Kinbara, T. Aida, *Nature* **2010**, *463*, 339; c) E. A. Appel, F. Biedermann, U. Rauwald, S. T. Jones, J. M. Zayed, O. A. Scherman, *J. Am. Chem. Soc.* **2010**, *132*, 14251.

[3] a) M. Hanack, M. Lang, *Adv. Mater.* **1994**, *6*, 819; b) R. J. M. Nolte, *J. Porphyr. Phthalocyanines* **2020**, *24*, 1243; c) S. Ogi, K. Sugiyasu, S. Manna, S. Samitsu, M. Takeuchi, *Nat. Chem* **2014**, *6*, 188. d) C. Zhang, P. Chen, H. Dong, Y. Zhen, M. Liu, W. Hu, *Adv. Mater.* **2015**, *27*, 5379; e) N. Sasaki, J. Kikkawa, Y. Ishii, T. Uchihashi, H. Imamura, M. Takeuchi, K. Sugiyasu, *Nat. Chem.* **2023**, *15*, 922.

[4] X. Zhong, A. Nagai, M. Takeuchi, J. Aimi, *Macromol. Rapid Commun.* **2023**, *44*, 2200666.

[5] a) V. Sathesh, J. K. Chen, C. J. Chang, J. Aimi, Z. C. Chen, Y. C. Hsu, Y. S. Huang, C. F. Huang, *Polymers* **2018**, *10*, 858; b) T. Y. Lin, C. W. Tu, J. Aimi, Y. W. Huang, T. Jamnongkan, H. Y. Hsueh, K. Y. A. Lin, C. F. Huang, *Nanomaterials* **2021**, *11*. 2392.

[6] a) T. Haino, N. Nitta, *ChemPlusChem* **2024**, *89*, e202400014; b) B. V. K. J. Schmidt, M. Hetzer, H. Ritter, C. Barner-Kowollik, *Polym. Chem.* **2012**, *3*, 3064; c) X. Y. Huan, D. L. Wang, R. J. Dong, C. L. Tu, B. S. Zhu, D. Y. Yan, X. Y. Zhu, *Macromolecules* **2012**, *45*, 5941; d) Z. Zhang, Q. Lv, X. Y. Gao, L. Chen, Y. Cao, S. J. Yu, C. L. He, X. S. Chen, *Acs Appl. Mater. Interfaces* **2015**, *7*, 8404; e) Y. Y. Liu, S. Lan, L. Q. Xiao, *Macromol. Chem. Phys.* **2015**, *216*, 749. f) B. V. K. J. Schmidt, D. Kugele, J. von Irmer, J. Steinkoenig, H. Mutlu, C. Ruttiger, C. J. Hawker, M. Gallei, C. Barner-Kowollik, *Macromolecules* **2017**, *50*, 2375. g) Z. Y. Hou, W. Dehaen, J. Lyskawa, P. Woisel, R. Hoogenboom, *Chem. Commun.* **2017**, *53*, 8423. h) N. Nitta, S. I. Kihara, T. Haino, *Angew. Chem. Int. Ed*. **2023**, *62*, e202219001.

[7] X. Zhong, D. Panigrahi, R. Hayakawa, Y. Wakayama, K. Harano, M. Takeuchi, J. Aimi, *J. Mater. Chem. C* **2024**, *12*, 9642.

[8] a) J. H. Zagal, S. Griveau, J. F. Silva, T. Nyokong and F. Bedioui, *Coord. Chem. Rev.* **2010**, 254, 2755; b) C. M. Lieber and N. S. Lewis, *J. Am. Chem. Soc.*, **1984**, 106, 5033.

[9] a) W. W. Kramer and C. C. L. McCrory, *Chem. Sci.* **2016**, 7, 2506; b) Y. Liu and C. C. L. McCrory, *Nature Commun.* **2019**, 10, 1683.

[10] a) J. Aimi, C.-T. Lo, H.-C. Wu, C.-F. Huang, T. Nakanishi, M. Takeuchi, W.-C. Chen, *Adv. Electron. Mater.* **2016**, *2*, 1500300; b) J. Aimi, P.-H. Wang, C.-C. Shih, C.-F. Huang, T. Nakanishi, M. Takeuchi, H.-Y. Hsueh, W.-C. Chen, *J. Mater. Chem. C* **2018**, *6*, 2724; c) J. Aimi, T. Yasuda, C.-F. Huang, M. Yoshio, W.-C. Chen, *Mater. Adv.* **2022**, *3*, 3128; d) D. Panigrahi, R. Hayakawa, X. Zhong, J. Aimi, Y. Wakayama, *Nano Lett.* **2023**, *23*, 319; e) R. Hayakawa, K. Takahashi, X. Zhong, K. Honma, D. Panigrahi, J. Aimi, K. Kanai, Y. Wakayama, *Nano Lett.* **2023**, *23*, 8339; f) Y. Shingaya, T. Iwasaki, R. Hayakawa, S. Nakaharai, K. Watanabe, T. Taniguchi, J. Aimi, Y. Wakayama, *ACS Appl. Mater. Interfaces* **2024**, *16*, 33796.

[11] M. Benaglia, J. Chiefari, Y. K. Chong, G. Moad, E. Rizzardo, S. H. Thang, *J. Am. Chem. Soc.* **2009**, *131*, 6914.

[12] T. Nyokong, *Polyhedron* **1995**, *14*, 2325.

[13] P. Kaur, S. D. Dogra, R. Sachdeva, R. Singh, S. Singh, S. K. Tripathi, G. S. S. Saini, *Mater. Today Proc.* **2020**, *21*, 1809.

[14] "Gibbs free energy changes ($\Delta G°$) of the supramolecular complexation at 298 K were estimated to be –18.7 kJ/mol for **CoPc**-**pyCTA** and –23.3 kJ/mol for **CoPcPS$_4$-pyPMMA**. Since the difference between these values was relatively small ($\Delta\Delta G°$ = 4.6 kJ/mol), there appeared to be no significant difference in coordination events with or without polymer chains."

[15] H. Zhang, G. K. K. Clothier, T. R. Guimarães, R. Kita, P. B. Zetterlund, Y. Okamura, *Polymer* **2022**, *240*, 124466.

[16] a) V. Sofonea, K. R. Mecke, *Eur. Phys. J. B* **1999**, *8*, 99; b) H. Wang, R. J. Composto, *Macromolecules* **2002**, *35*, 2799.

Entry for the Table of Contents

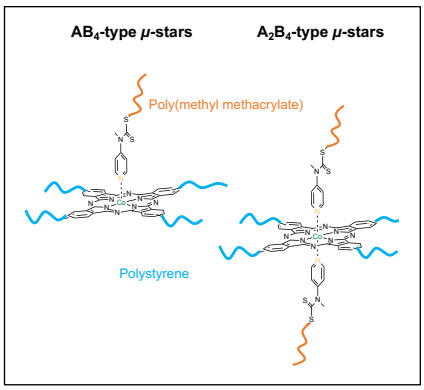

Metal-ligand coordination has been used to generate a supramolecular miktoarm star-shaped copolymer with a cobalt(II) phthalocyanine (CoPc) core. Stepwise axial coordination of the terminal pyridyl group of poly(methyl methacrylate) to the CoPc core of the four-armed, star-shaped polystyrene provided AB_4- and A_2B_4-type microstars.